N82 23467

Effects of rotation and magnetic field on the onset of convective instability in a liquid layer due to buoyancy and surface tension

Gabbita Sundara Rama Sarma

Institut für Theoretische Strömungsmechanik,
Deutsche Forschungs- und Versuchsanstalt für Luft- und Raumfahrt
Bunsenstrasse 10, D-3400 Göttingen, Federal Republic of Germany

Abstract

Thermocapillary stability characteristics of a horizontal liquid layer heated from below rotating about a vertical axis and subjected to a uniform vertical magnetic field are analyzed under a variety of thermal and electromagnetic boundary conditions. Results based on analytical solutions to the pertinent eigenvalue problems are discussed in the light of earlier work on special cases of the more general problem considered here to show in particular the effects of the heat transfer, nonzero curvature and gravity waves at the two-fluid inferface. Although the expected stabilizing action of the Coriolis and Lorentz force fields in this configuration are in evidence the optimal choice of an appropriate range for the relevant parameters is shown to be critically dependent on the interfacial effects mentioned above.

Introduction

In recent years there has been a resurgence of interest in understanding the origins and possible means of controlling convective instability, especially in configurations relevant to material sciences in general and material processing in particular within the framework of the current space programs. In this context some of the basic aspects of this problem area have been under investigation[1-4] by the present author. The contribution to be presented here is part of a continuing effort at the DFVLR to analyze some of the basic fluid dynamic aspects relevant to the material science configurations, especially in the context of space experiments under reduced gravity conditions and the related ground based research.

Since references [1-4] give the general background and motivation for the particular problem considered here and cite the relevant literature, we shall restrict ourselves here only to a resport of some of the recent results obtained and discuss them in the light of those available in the literature. While references 1-4 deal exclusively with the zero gravity situation, we consider here specifically the simultaneous action of surface tension and gravity in this classical Bénard - Marangoni configuration.

Formulation of the problem

We consider an infinite, horizontal, Boussinesq liquid layer of mean thickness d rotating about a vertical axis at a constant angular speed Ω and subjected to a uniform magnetic induction field of strength B_0 under various typical boundary conditions to be detailed later. Figure 1 illustrates the configuration schematically and is followed by a list of the symbols for dimensional quantities occurring in the later development. The details of the formulation incorporate the features introduced by Scriven and Sternling [5] and Smith [6] extending the pioneering work of Pearson[7].

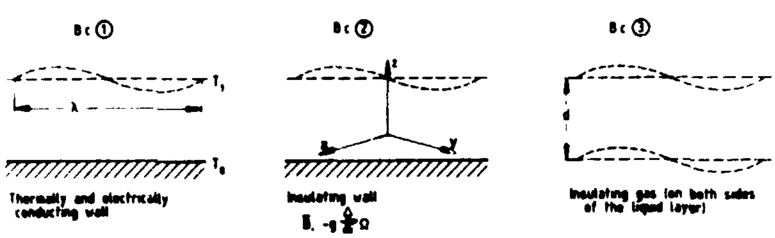

Figure 1. The Bénard - Marangoni configuration

List of symbols

β = Coefficient of thermal volume expansion, $-\frac{1}{\rho}\frac{\partial\rho}{\partial T}$
γ = Electrical conductivity
ΔT = Applied temperature difference $(T_0 - T_1)$
ζ_0 = Amplitude of the disturbance wave at the two-fluid interface
η_m = Magnetic diffusivity $(\gamma\mu_m)^{-1}$
κ = Thermal diffusivity, $K/\rho c_0$
λ = Disturbance wavelength, $2\pi/\sqrt{k_x^2+k_y^2}$
μ = Dynamic viscosity
μ_m = Magnetic permeability
ν = Kinematic viscosity
ρ = Density
σ = Interfacial energy at the two-fluid interface
Ω = Angular speed of rotation
$\vec{B}$ = Magnetic induction field
B_0 = Magnitude of the applied $\vec{B}$-field
K = Thermal conductivity
T = Temperature
c_0 = specific heat
d = Mean thickness of the liquid layer
g = Acceleration due to gravity
h = heat transfer coefficient at the disturbed interface
k_x, k_y = Disturbance wave numbers in the x-y-directions
p = Time constant in the exponential growth/decay factor of a disturbance normal mode

The liquid layer has nominally constant temperatures T_0, T_1 $(T_0 > T_1)$ respectively at its lower and upper horizontal boundaries. For the sake of definiteness and simplicity the characteristics of the adjoining media are somewhat idealized. They are specified for the three cases ①, ②, ③ of the boundary conditions (b.c.) as follows.

In b.c. ① we take the bottom boundary as a thermally and electrically perfect solid conductor. In b.c. ② the bottom boundary is a thermally and electrically perfect insulator. In both cases the upper adjoining medium is taken as an electrically insulating gas extending in the z-direction to infinity. The heat transfer to the gas from the liquid layer can be simplified (without going into the details of the possible flow in the upper medium) in terms of an effective heat transfer coefficient h(T)[5,7] for the two-fluid interface. A detailed discussion of this simplification was given by Pearson[7]. In b.c. ③ we consider the situation where the same ambient gas is present on both sides of the liquid layer.

The onset of convective instability in such a liquid layer with an initially uniform linear temperature profile can be formulated as a linear eigenvalue problem for the disturbance amplitudes of the flow variables using the standard normal modes procedure[8]. We non-dimensionalize the problem using[5,8] d, d^2/ν, κ/d, κ/d^2, $4\pi\gamma\kappa B_0/d$, ΔT respectively as the reference quantities for length, time, velocity, vorticity, electric current density and temperature. The stability of the configuration with respect to an infinitesimal normal mode of disturbance may then be stated in terms of the following eigenvalue problems in dimensionless form.

$$(D^2-a^2)(D^2-a^2-p_2)(D^2-a^2-p_1)W - Ta(D^2-a^2-p_2)DZ - Q(D^2-a^2)D^2W = Ra \cdot a^2(D^2-a^2-p_2)\theta \tag{1}$$

$$(D^2-a^2-p_3)\theta + W = 0 \tag{2}$$

$$(D^2-a^2-p_1)Z + Ta \cdot DW + QDX = 0 \tag{3}$$

$$(D^2-a^2-p_2)X + DZ = 0 \tag{4}$$

where $D \equiv (1/d) \cdot d/dz$ and W, Z, X, θ are respectively the dimensionless disturbance amplitudes of the z-components of velocity, vorticity and electric current density and of temperature.

The boundary conditions are to distinguish not only between cases ①, ②, ③ specified earlier but also as to whether the neutrally stable oscillatory $(p_1 \neq 0)$ or stationary $(p_1 = 0)$ modes are considered while determining the stability boundary for the configuration.

(a) Neutral modes oscillatory $(p_1 \neq 0)$

B.c. ① $$W(0) = 0 = DW(0) = \theta(0) = Z(0) = DX(0) \tag{5}$$

B.c. ② $$W(0) = 0 = DW(0) = D\theta(0) = Z(0) = X(0) \tag{6}$$

B.c. ③ $$W(0) = \frac{p_3\zeta_0}{d} \quad \text{(Kinematic condition at the two-fluid interface)} \tag{7}$$

For $Nu = \frac{hd}{K\Delta T} \neq 0$

$$\frac{Cr}{(Bo+a^2)}\left\{(D^2-p_1-3a^2)DW(0)\right\} - \left\{\frac{D\theta(0)}{Nu} + \theta(0)\right\} = 0 \tag{8}$$

$$(D^2+a^2)W(0) - \frac{a^2 \cdot Ma\, D\theta(0)}{Nu} = 0 \tag{9}$$

For Nu = 0

$$D\theta(0) = 0 \tag{10}$$

$$\frac{p_3 Cr}{a^2(Bo+a^2)} \{ (D^2-3a^2-p_1)DW(0) \} - W(0) = 0 \tag{11}$$

$$p_3(D^2+a^2)W(0) + Ma \cdot a^2 \{ p_3\theta(0)-W(0) \} = 0 \tag{12}$$

B.c. at $z=d$ for cases ①, ②, ③ are of the same form as those for case ③ at $z=0$.

(b) Neutral modes stationary ($p_1 = 0$)

The conditions (11),(12) above are to be replaced by

$$W(0) = 0 \quad \text{(which covers also (7) above)} \tag{13}$$

$$D^2W(0) + a^2 \cdot Ma\theta(0) + \frac{Ma \cdot Cr}{(Bo+a^2)} \{ -D^3W(0) + 3a^2 DW(0) \} = 0 \tag{14}$$

Again the b.c. at $z=d$ are of the same form for cases ①, ②, ③ as those for case ③ at $z=0$.

The dimensionless numbers occurring in the above formulation are $Bo = \rho g d^2/\sigma$ (Bond), $Cr = \kappa\mu/\sigma d$ (crispation), $Ma = |(\partial\sigma/\partial T)\Delta T|/\mu\kappa$ (Marangoni), $Nu = dh/K\Delta T$ (Nusselt), $Pr = \nu/\kappa$ (Prandtl), $Pr_m = \nu/\eta_m$ (magnetic Prandtl), $Q = B_0^2 d^2 \gamma/\mu$ (Chandrasekhar), $Ra = g\beta\Delta T d^3/\nu\kappa$ (Rayleigh) $Ta = 2\Omega d^2/\nu$ (Taylor), $a = 2\pi d/\lambda$ (disturbance wave number), $p_1 = pd^2/\nu$ (frequency factor for oscillatory disturbance mode), $p_2 = Pr_m \cdot p_1$, $p_3 = Pr \cdot p_1$. The last four parameters are characteristics of a disturbance normal mode in the hydromagnetic thermocapillary stability discussion of the configuration whereas the first nine describe the basic configuration.

Briefly[5,6] the boundary conditions (5),(6) state the no-slip condition and the thermal and electromagnetic properties associated with the boundaries whereas (8),(9) cover the requirements[5,6] of stress balance along and normal to the two-fluid interface incorporating the thermocapillary terms and also taking into account the nonzero interfacial curvature (Cr), gravity waves (Bo) and heat transfer contribution at the disturbed interface (Nu).

The existence of oscillatory modes in this configuration especially at large Ta is well-known for the buoyancy-driven case[8] and was also demonstrated in the surface tension-driven case. The oscillatory modes become important at low Pr but it was found[1] that at least for $Bo = 0$ the incipient instability is stationary rather than oscillatory since the corresponding critical Marangoni number is higher than that for the stationary mode which is independent of Pr. It turns out that for small $Bo \neq 0$ the critical Ma_c tends to decrease and $a_c \to 0$ with large Ta whereas the oscillatory modes were shown by asymptotic analysis[1] to occur at large $Ma_c \sim Ta \gg 1$, as a short wave instability with $a \sim \sqrt{Ta}$. Thus we have some plausible evidence to suppose that in this configuration, where the effects of the magnetic field ($Q \neq 0$) which inhibits the onset of buoyancy-driven oscillatory modes (for $Pr > Pr_m$)[8] are also included, the stationary modes precede the oscillatory ones at onset of instability

Since the practical interest in the present investigation lies ultimately in the suppression of convective instability[1-4] we consider here the case $p_1 = 0$ in the following. If, however, the solution of the complete eigenvalue problem with $p_1 \neq 0$ posed above does lead to oscillatory modes we have then only to compare the corresponding minimum critical Marangoni number with Ma_c computed here. Ma_c is in any case an upper bound for stability of the configuration.

The stationary modes of convective instability are given by nontrivial solutions to the homogeneous boundary value problems given by (1) - (10), (13), (14) for the different cases ①, ②, ③. The secular conditions for the existence of nontrivial solutions to the respective homogeneous boundary value problems have been obtained by using the exact analytical solutions (combinations of trigonometric and hyperbolic functions) of (1) - (4) in the appropriate boundary conditions. The neutral stability characteristics of the configuration are then analyzed from the resulting transcendental secular relationship in terms of the dimensionless parameters of the problem. Since we have a large number of dimensionless groups here, we shall have to choose a suitable range of their values with some class of applications in view. As indicated in references[1-4] the interface curvature effects are already in evidence for such small values of $Cr = 10^{-3}, 10^{-4}$ yielding stability characteristics quite different from those for $Cr = 0$. Using the thermophysical property data available in the literature[9-11] the parameter ratio $Bo/Cr = gd^3/\nu\kappa$ at $g = 9.81\,m/s^2$ with $d = mm$ has values of $0(10^2)$ as shown in Table 1 for some substances of interest

Table 1. Typical values for Bo/Cr

Silicone oil (Dow-Corning 200)	Cu-melt	Al-Cu-melt	Ga As-melt	Si-melt
4.5×10^2	6.07×10^2	5.1×10^2	7.1×10^2	1.82×10^3

The corresponding values for different levels of gravity and the appropriate size of the layer for experiments in space missions can be estimated from Table 1. We can also use them for estimating parameters such as Ra and Bo say by choosing $Cr = 10^{-3}$, 10^{-4} to demonstrate the effects of nonzero interfacial curvature. It is found that $Cr = 10^{-3}$, 10^{-4} for Silicone oil (Dow-Corning 200) [10], used frequently for convection experiments, when d = mm, cm respectively. Thus for experiments in a terrestrial laboratory in the mm size and in an orbital laboratory in the cm range can be covered by considering $Bo = 0.05$, 0.5 and $Cr = 10^{-3}$, 10^{-4} to emphasize the effects of interfacial waves. Table 2 gives some representative values for Q and Ta.

Table 2. Values of Q at $B_0 = 0.5$ tesla and Ta at $\Omega = 500$ rpm for d = mm

	Silicone oil DC 200	Al-melt	GaAs-melt	Si-melt	Cu-melt
Q	—	9.02×10^2	5.57×10^2	1.14×10^2	8.43×10^2
Ta	0.524	1.95×10^2	3.37×10^2	2.98×10^2	2.48×10^2

Results and discussion

The eigenvalue relationships giving the stability characteristics of the present configuration under b.c. ①, ②, ③ have been obtained by investigating various special cases: $Ta = 0$, $Q \neq 0$; [4] $Ta \neq 0$, $Q = 0$; [3] $Ta, Q \gg 1$; [2] $Ta \gg 1$, $Q = 0$, $p_1 \neq 0$ [1] all with $Ra = 0 = Bo$ i.e., under zero gravity bringing out the essential differences between $Cr = 0$ and $Cr \neq 0$.

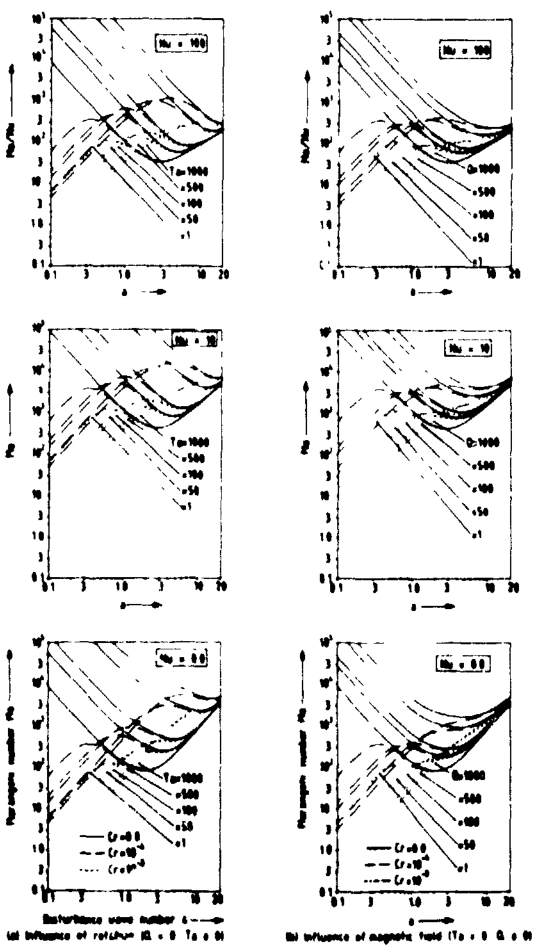

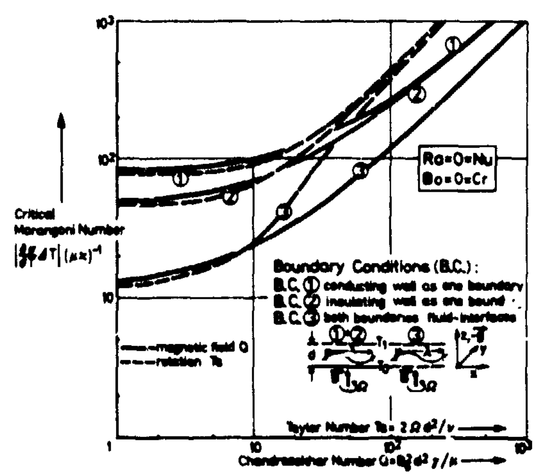

Figure 3. Variation of Ma_c with rotation (Ta) and magnetic field (Q) neglecting interfacial effects ($Cr = 0 = Nu$) under zero gravity for b.c. ①, ②, ③.

Figure 2. Neutral stability curves for the onset of thermocapillary convective instability in a liquid layer under zero gravity: Effects of interfacial curvature (Cr) and heat transfer (Nu) under the influence of (a) rotation alone and (b) magnetic field alone for b.c. ①.
The unstable domain is above the respective curves.

ORIGINAL PAGE IS
OF POOR QUALITY

Figure 2 shows the neutral stability curves of the present configuration under the action of (a) rotation alone and (b) magnetic field alone for different Nu, Cr at Bo = 0 = Ra for b.c. ①. We notice first of all the radical departure of the stability characteristics for $Cr \neq 0$ from those of Cr = 0, namely, that there exists strictly speaking no minimum critical Marangoni number when $Cr \neq 0$ as was first shown by Scriven and Sternling[5] for Ta = 0 = Q. Asymptotic analysis in the limit $a \to 0$ shows that $Ma \sim f(Ta,Q)(Nu+1)/a^2, a \to 0$ for Cr = 0 whereas $Ma \sim g(Ta,Q)(Nu+1)a^2/Cr$, $a \to 0$ for $Cr \neq 0$ under b.c. ①. The numerical results shown confirm this limiting behaviour as well (note the linearity of the curves for small a). The above formulas incidentally include the factor (Nu+1) missing in those of reference 5 (Table 1, p.333) for Ta = 0 = Q.

For sufficiently small Cr/g(Ta,Q) we may speak of a quasi-critical Marangoni number Ma_c which is approximately equal to that calculated using Cr = 0 in earlier literature[1,2,13]. Since the unstable long wave band increases in size with Ta and Q (for $Ta \gg 1$, $Q \ll 1$; $Ta \ll 1$, $Q \gg 1$ respectively the corresponding band widths are $0(Cr\sqrt{Ta})$ and $0(Cr\sqrt{Q})$, Cr must indeed accordingly be smaller for this approximation to hold at higher Ta, Q. As shown in Figure 2 the effects of heat transfer ($Nu \neq 0$) at the two-fluid interface are stabilizing in that the unstable domain is pushed upward along the Ma - axis with increasing Nu.

Figure 3 shows the monotonically increasing stabilization potentially to be achieved by increasing rotation (Ta) and magnetic field (Q) under the three typical b.c. ①, ②, ③ which, it may be noted, are in decreasing order of stability amongst themselves. The results shown agree with those in references 12,14 for Cr = 0. Asymptotically $Ma_c = 0(Q)$ for $Q \gg 1$, $Ta \ll 1$ and $Ma_c = 0(Ta)$ for $Ta \gg 1$, $Q \ll 1$. Note that the asymptotic range is attained faster by Ta than by Q due to the influence of rotation on the flow field in general and vorticity in particular. The differences between the b.c. persist longer in the case of magnetic field. The situation is analogous in the case of buoyancy[8]

Apart from their formal interest the results shown in Figures 2, 3 for Cr = 0 may also be seen as useful approximations for sufficiently small Cr and at low levels of gravity provided the long wave instabilities are considered relatively harmless. The relevant ranges of the parameters will become apparent in the later discussion.

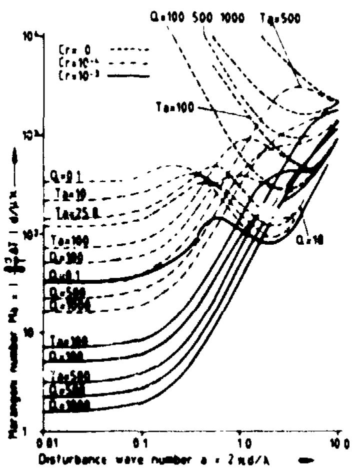

Figure 4. Neutral stability curves for b.c. ① with Nu = 0. Bo = 0.05 at low gravity (Ra = 0.1) for different Ta (Q = 0.1) and Q (Ta = 0.1)

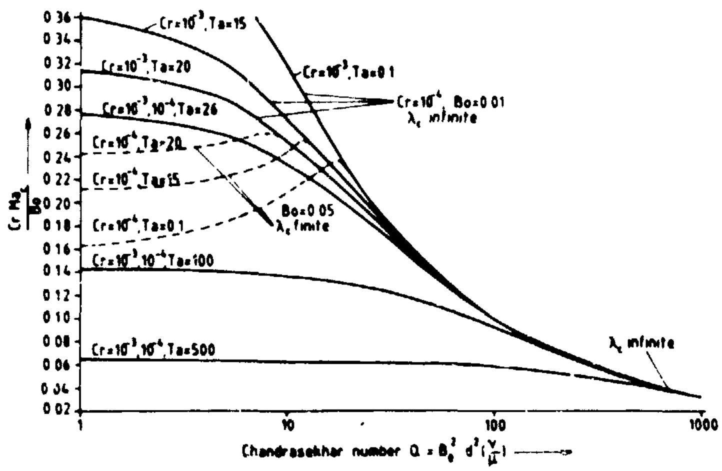

Figure 5. Correlation of the critical Marangoni number Ma_c with Bo/Cr for b.c. ① with Nu = 0, Ra = 0.1 at Cr = 10^{-3}, 10^{-4}; Bo = 0.01, 0.05

Figure 4 shows the further departure of the stability characteristics of the configuration from those at Cr = 0 when we consider low Bond number and crispation effects together. We notice first of all the reinstatement of an absolute minimum critical Ma_c for the onset of convective instability as was first shown by Smith[6] for Ta = 0 = Q. The neutral stability curves for Cr = 10^{-4} show two minima, one at a = 0 and the other at finite a. Even for Cr = 10^{-3} the same feature can be reproduced at Bo = 0.5. This is due to the fact that the long wave stability characteristics depend on the ratio Bo/Cr and not individually on Bo, Cr. The occurrence of double minima has been confirmed for Bo/Cr ≥ 200. The lesser of the two minima is then the critical Ma_c for the onset of instability. For small Ta(<25.8) and small Q(<18) we observe that the critical wavelength λ_c corresponding to Ma_c is finite whereas at higher Ta and Q, λ_c is infinite at onset of instability. It may also be mentioned that when λ_c is finite it does correspond to the value for $Cr = 0$. Ma_c clearly decreases monotonically with larger Ta,Q and the corresponding λ_c is then infinite. Thus, allowing for gravitational waves and crispation effects leads to long wave instability at a low but finite Ma_c for large Ta and Q.

Figure 5 shows the correlation of Ma_c with Bo/Cr for b.c. 1 with $Nu = 0$, $Ra = 0.1$ at $Cr = 10^{-3}, 10^{-4}$; $Bo = 0.01, 0.05$. Along the continuous parts of the curves λ_c is infinite and along the broken ones λ_c is finite. The latter situation is found to occur at low Ta(<25.8) and $Q < Q^*$ ($Q^* = 18, 12, 8.5$ respectively for $Ta = 0.1, 15, 20$) and large enough Bo/Cr. The last provision is to be recognized along the curves for $Ta < 26$ where the respective curves split off at Q^* into two branches applying separately for $Bo = 0.01$ ($\lambda_c \to \infty$) and $Bo = 0.05$ (λ_c finite) eventhough both correspond to the same value of $Cr = 10^{-4}$. For large enough Ta and Q values the correlation with Bo/Cr is universal and $a_c = 0$. Furthermore we notice that at large $Q(\sim 800)$ all the curves for $Ta \leq 500$ merge. This implies a certain "saturation effect" as far as the influence of rotation is concerned while acting together with the magnetic field as a stabilizing agent.

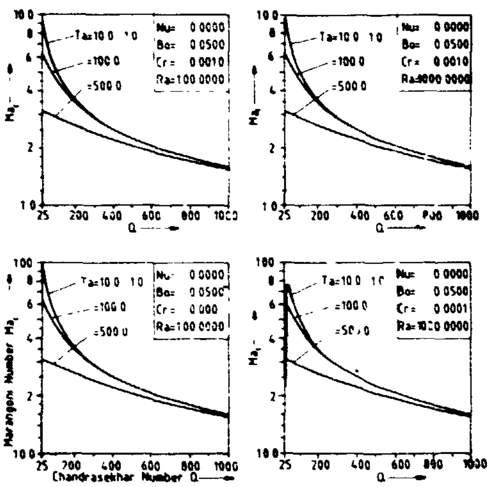

Figure 6. Variation of Ma_c with rotation (Ta) and magnetic field (Q) for b.c. 1 with $Nu = 0$

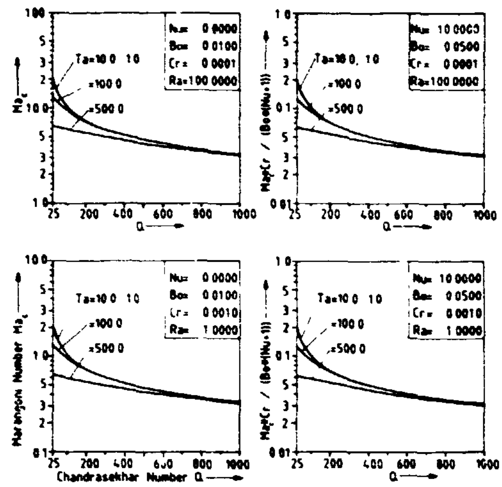

Figure 7. Variation of Ma_c with Bo, Cr, Nu for b.c. 1

Figure 6 shows the variation of Ma_c with Ta and Q (≥ 25) wherein the monotonic decrease of Ma_c is to be noted even for $Bo/Cr = 500$ in contrast to the initial increase observed in Figures 4, 5 for lower Ta, Q. (In Figures 6 - 8 the respective constant parameter values are indicated in the inset.). The computations show that Ma_c hardly changes with Ra. In fact for $Cr = 10^{-3}$, $Bo = 0.05$ the upper right quadrant of Figure 6 shows that even up to $Ra = 1000$, Ma_c is that given by the long wave limit $(Ma)_{a=0}$. However for higher Bo/Cr (=500 shown) the buoyancy effects become noticeable from $Ra > 300$ for $Ta = 0.1$, 10 at $Q = 25$ since now Q^* increases for $Ta = 0.1$, 10 from 18, 12 respectively at low Ra (= 0.1) to 47, 46 at moderate Ra (= 1000). This is indicated in the lower right hand quadrant of Figure 6. This latter range, where buoyancy effects become noticeable, is distinguished by the broken curve along which λ_c is finite. (The curves for $Ta = 0.1$, 10 are hardly to distinguish on the scale drawn but they end, when extended, respectively at approximately $Q_0 = 16.5$ and 13.2 on the Q-axis.)

Figure 7 shows the correlation of Ma_c with (Bo/Cr) (Nu+1) f (Ta, Q) for different combinations of Bo, Cr, Nu. The coefficient functions f (Ta, Q) shown have been confirmed numerically for various combinations of the parameters as long as the buoyancy effects are not noticeable. The "universality" of these correlation functions depends slightly on the parameter range but is found to be within a few percent at $a = 0.02$ chosen to represent the limit $a \to 0$. Another feature to be noted from Figures 4 - 7 is that $a_c \to 0$ as Ta, Q increase and $a_c = 0$ for all Ta, Q greater than some not too large a value. This is in contrast to the common finding of the earlier studies [12-14] (wherein Cr was set equal to zero a priori), namely, that a_c increases with Ta and Q. Here we see that as long as the buoyancy effects do not dominate, the stationary form of instability sets in only at $a_c = 0$ for sufficiently large Ta and Q.

Now we turn to the effect of the boundary conditions on the stability characteristics of the configuration. In all the three cases of b.c. 1, 2, 3 the same trends in the variation of Ma_c are observed for low Ra. Ma_c is proportional to Bo/Cr and decreases monotonically with Ta, Q for low Bo/Cr as demonstrated in Figure 8(a) for Bo/Cr = 10, 100.

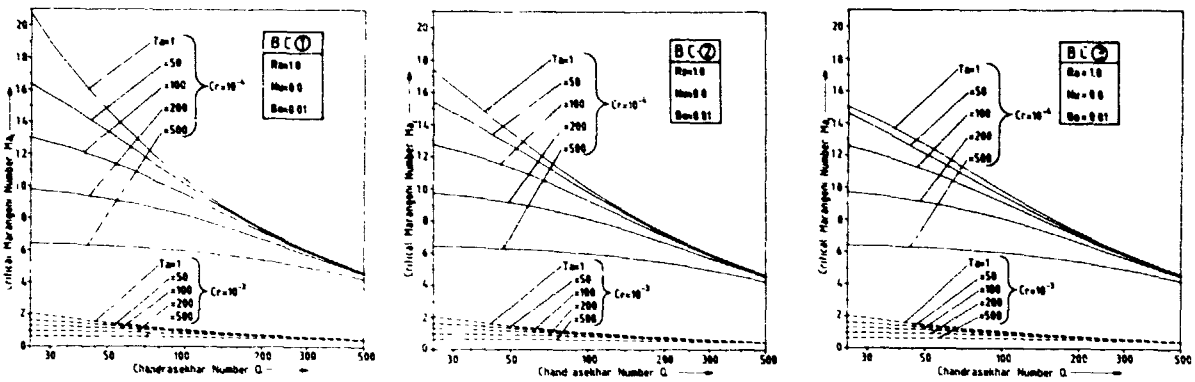

Figure 8(a). Effect of boundary conditions on the variation of Ma_c at Bo/Cr = 10, 100

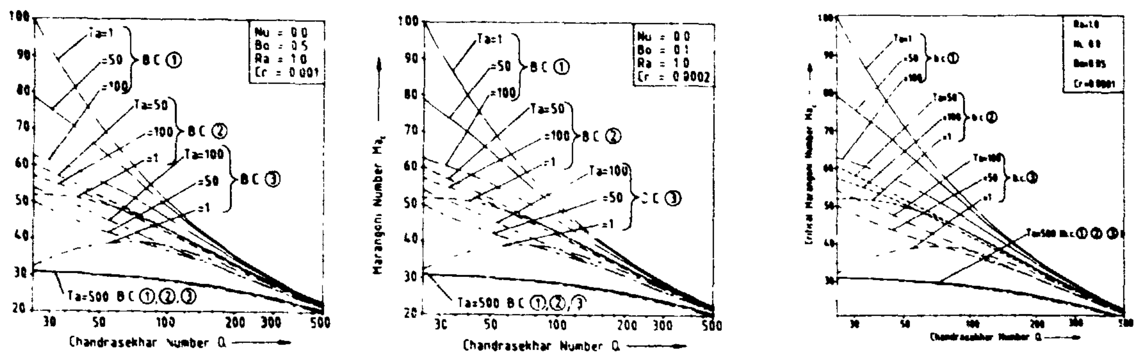

Figure 8(b). Effect of boundary conditions on the variation of Ma_c at Bo/Cr = 500

We also note that at low Ta and Q, Ma_c for b.c. ① is higher that that for b.c. ② and the latter in turn is higher than that for b.c. ③. This indicates the decreasing degree of stability imparted by the degrees of freedom allowed by the three types of boundary conditions ①, ②, ③ in that order. This feature is similar to that for the buoyancy-driven convective instability [8] although the boundary conditions there are different. For large Ta and Q, however we notice (cf. Q >500, or Ta = 500) the boundary conditions can no longer be distinguished from each other. In the present case the role of the b.c. is further enhanced via the dependence on Bo/Cr. The lower Bo/Cr, the lesser is the influence of b.c. even at low Ta,Q (cf. Ta = 1,50 for Bo = 0.01, Cr = 10^{-3} shown by dashed curves in the lower part of Figure 8(a).)

Complementary to the results in Figure 8(a) those in 8(b) demonstrate that for larger Bo/Cr (= 500 for three different combinations of Bo,Cr) a more pronounced effect of the boundary conditions on the variation of Ma_c and in particular that Ma_c can decrease as well as increase with Ta and Q depending on the range of parameters. Again at large Ta, Q the distinction between the boundary conditions decreases.

Conclusions

The onset of stationary convective instability driven by both density- and surface-tension-gradients in a horizontal liquid layer heated from below can be suppressed by means of rotation about a transverse axis and by a transverse magnetic field. But the stabilizing influence of these two agencies is subject to considerable qualifications in view of the effects of curvature and gravity waves at the two-fluid interface. The larger the ratio Bo/Cr, the greater the range of stabilizing action in terms of Ta, Q for all the boundary conditions considered and relatively greater for b.c. ② and ③ than for b.c. ①. The influence of the individual b.c. ①, ②, ③ becomes indistinguishable at larger Ta, Q and at lower Bo/Cr. Since Ma_c decreases with Ta, Q (for sufficiently large Ta, Q) and $a_c \to 0$, an optimal parameter range for the combined stabilizing action of rotation and magnetic field must be sought appropriately. Allowance for heat transfer he ambient gas is generally stabilizing.

In the low gravity situation (small Bo and Ra < 100) the buoyancy effects do not perceptibly influence the onset of instability except at low Ta and Q. In this range the onset of instability is at a finite wave number $a_c \neq 0$ which is independent of Bo, Cr as may be expected. (Ma_c corresponds otherwise to $a_c = 0$ and as shown ∝ Bo/Cr for Nu = 0.) The general problem of interaction between buoyancy and surface tension will be considered in a later report but it seems legitimate to draw a partial conclusion on the basis of results shown here, namely, that the buoyancy-dominated situation tends to prefer finite wave length instability while the capillarity-dominated situation including the effects of interfacial curvature and interfacial gravity waves tends to favour the infinitely long wave mode of instability. This conclusion is qualitatively in constrast to that of earlier studies on this configuration ignoring the interfacial effects altogether (Bo = 0 = Cr). This stems only from the nonzero Bo/Cr and does not explicitly depend on the (finite) value of the mean surface tension [1-5].

The question of oscillatory modes of instability has been bypassed here on the basis of asymptotic results indicating that the incipient instability is stationary for large Ta(Q = 0). The results for the finite range of Ta and Q need of course to be examined in order to confirm whether Ma_c calculated here is indeed the absolute minimum critical Marangoni number for the onset of instability.

References

1. Sarma, G.S.R., "On Oscillatory Modes of Thermocapillary Instability in a Liquid Layer Rotating about a Transverse Axis", Physico Chemical Hydrodynamics (in Press), 1981.
2. Sarma, C.S.R., "Marangoni Convection in a Liquid Layer under the Simultaneous Action of a Transverse Magnetic Field and Rotation", Adv. Space Res., Vol. 1, pp. 55-58. 1981.
3. Sarma, G.S.R., "Marangoni Convection in a Liquid Layer Subjected to Rotation about a Transverse Axis", Proc. 3rd European Symp. on Material Sciences in Space, Grenoble 24-27 April 1979, - ESA SP-142, pp. 359-362. 1979.
4. Sarma, G.S.R., "Marangoni Convection in a Fluid Layer under the Action of a Transverse Magnetic Field", Space Research, Vol. XIX, pp. 575-578. 1979.
5. Scriven, L.E. and Sternling, C.V., "On Cellular Convection Driven by Surface-Tension Gradients: Effects of Mean Surface Tension and Surface Viscosity", J. Fluid Mech., Vol. 19, pp. 321-340. 1964.
6. Smith, K.A., "On Convective instability Induced by Surface-Tension Gradients", J. Fluid Mech., Vol. 24, pp. 401-414. 1966.
7. Pearson, J.R.A., "On Convection Cells Induced by Surface Tension", J. Fluid Mech., Vol. 4, pp. 489-500. 1958.
8. Chandrasekhar, S., Hydrodynamic and Hydromagnetic Stability, Oxford University Press 1961.
9. Bourgeois, S.V., "Buoyant and Capillary Natural Convection in Infinite Horizontal Liquid Layers Heated Laterally", Letters in Heat and Mass Transfer, Vol. 2, pp. 223-236. 1975.
10. Palmer, H.J. and Berg, J.C., "Convective Instability in Liquid Pools Heated from Below", J. Fluid Mech., Vol. 47, pp. 779-787. 1971.
11. Chang, C.E. and Wilcox, W.R., "Inhomogeneities due to Thermocapillary Flow in Floating Zone Melting", J. Crystal Growth, Vol. 28, pp. 8-12. 1975.
12. Nield, D.A., "Surface Tension and Buoyancy Effects in the Cellular Convection of an Electrically Conducting Liquid in a Magnetic Field", ZAMP, Vol. 17, pp. 131-139. 1966.
13. Namikawa, T., Takashima, M. and Matsushita, S., "The Effect of Rotation on Convective Instability Induced by Surface Tension and Buoyancy", J. Physical Soc. Japan, Vol. 28, pp. 1340-1349. 1970.
14. Vidal, A. and Acrivos, A., "The Influence of Coriolis Force on Surface-Tension-Driven Convection", J. Fluid Mech., Vol. 26, pp. 807-818. 1966.